Green Synthesis and Multi-Technique Structural–Optical Evaluation of ZnO/NiO Nanocomposite for Optoelectronic Applications

Akumarti Raju[1], Vangapandu Anusha[1], Gattupalli Manikya Rao[1]*, Budithi Ravi Kumar[1]*

[1]Department of Physics, Andhra University, Visakhapatnam, Andhra Pradesh 530003, India.

Abstract

This work demonstrates a straightforward, inexpensive, and rapid route for the synthesis of nickel oxide (NiO), Zinc Oxide (ZnO), and its composite (ZnO/NiO) nanoparticles through the green method using ***Azadirachtaindica*** (Neem) leaves. ZnO, NiO, and ZnO/NiO nanostructures were synthesized through an eco-friendly green route and comprehensively characterized to understand their structural and optical behaviors. TEM and HRTEM analyses revealed well-defined nanocrystalline domains with lattice fringes corresponding to ZnO (002) and NiO (111) planes, confirming successful formation of a ZnO–NiO heterojunction. FTIR spectra showed distinct Zn–O and Ni–O stretching vibrations along with phytochemical-derived surface functionalities, while the composite displayed merged metal–oxygen bands indicative of strong interfacial interaction. Raman spectroscopy identified characteristic ZnO E_2 modes and defect-activated NiO phonons, with the composite exhibiting combined and slightly shifted peaks due to phonon coupling at the interface. Photoluminescence measurements demonstrated near-band-edge and defect emissions for ZnO and NiO, whereas the ZnO/NiO nanocomposite showed blue-shifted peaks with significantly reduced intensity, confirming suppressed electron–hole recombination and enhanced charge separation. Overall, the integrated structural and optical results highlight the effectiveness of green synthesis in producing high-quality ZnO/NiO heterostructures with promising potential for optoelectronic and energy-related applications.

Key words: Green Synthesis, ZnO/NiO NPs, Transmission Electron Microscope, FTIR, Raman spectroscopy, Photoluminescence spectroscopy.

Corresponding Author:

***Dr. Gattupalli Manikya Rao**

***Dr. Budithi Ravi Kumar**

1. Introduction:

Metal-oxide nanomaterials have emerged as highly versatile materials for applications in photocatalysis, optoelectronics, sensors, and energy storage due to their tunable electronic structures, abundant defect chemistry, and excellent thermal and chemical stability [1]. Among these, zinc oxide (ZnO), a wide-bandgap n-type semiconductor, and nickel oxide (NiO), a p-type semiconductor with rich redox behavior, are particularly attractive because their structural and optical properties can be engineered at the nanoscale to enhance charge-transport and light–matter interactions [2]. When combined, ZnO and NiO form a p–n heterojunction, which significantly improves interfacial charge separation, suppresses recombination, and enhances catalytic and electrochemical performance—features highly valuable for modern energy-related devices [3].

The synthesis method plays a critical role in determining the quality, crystallinity, defect distribution, and environmental compatibility of such nanomaterials. Conventional chemical synthesis routes often rely on harsh reducing agents and toxic precursors. In contrast, green synthesis using plant extracts provides a sustainable and eco-friendly approach, where phytochemicals such as polyphenols, flavonoids, and organic acids act as natural reducing, stabilizing, and capping agents [4]. This bio-mediated method not only reduces environmental impact but also introduces unique surface functionalities and defect states that can positively influence optical and electronic behavior.

In this study, we report the green synthesis of ZnO, NiO, and ZnO/NiO nanocomposites and systematically investigate their structural, vibrational, and optical properties using TEM, FTIR, Raman, and PL techniques. The results collectively demonstrate that the ZnO/NiO heterostructure exhibits improved crystallinity, strong interfacial coupling, modified phonon behavior, and reduced electron–hole recombination [5] These enhancements highlight the potential of green-synthesized ZnO/NiO nanocomposites as efficient candidates for energy-related technologies.

2. Experimental

2.1 Materials

Azadirachtaindica (Neem) leaves, Zinc acetate dihydrate ($Zn(CH_3CO_2)_2 \cdot 2H_2O$), Nickel acetate dihydrate ($C_4H_{12}NiO_6$) and Sodium Hydroxide (NaOH). All the chemicals were used as received without any further purification.

2.2 Green synthesis of ZnO, NiO, and ZnO/NiO nanocomposite

ZnO, NiO, and ZnO/NiO nanocomposites were fabricated through an environmentally benign green synthesis approach adapted from Saravanan et al., employing plant-derived phytochemicals as natural reducing and stabilizing agents in place of hazardous chemicals. Fresh *Azadirachta indica* (Neem) leaves were collected, thoroughly washed with tap and distilled water to remove dust and surface contaminants, and subsequently dried in a hot-air oven at 35 °C for 2 h. Approximately 10 g of the dried leaves were then boiled in 100 mL of distilled water at 70 °C for 30 min to extract bioactive components. The mixture was filtered using Whatman filter paper, and the obtained leaf extract was stored at 4 °C for later use.

For the preparation of the ZnO/NiO nanocomposite, 25 mL of the stored leaf extract was combined with 50 mL of distilled water and stirred at 60 °C for 30 min. Separately, 0.2 M zinc acetate dihydrate and 0.2 M nickel acetate dihydrate solutions were prepared and added to the extract-containing mixtures under continuous stirring. To ensure homogeneous precursor interaction, the zinc solution was gradually introduced into the nickel solution while maintaining constant agitation. The pH of the reaction mixture was adjusted to ~7 using 0.5 M NaOH, and the suspension was stirred for an additional 6 h to facilitate complete co-precipitation. The obtained precipitate was centrifuged at 3500 rpm for 10 min, repeatedly washed with distilled water and ethanol to eliminate unreacted residues, and dried at 60 °C for 6 h. Finally, the dried powder was annealed at 500 °C for 2 h in a programmable furnace to form the ZnO/NiO nanocomposite. Pure ZnO and NiO samples were synthesized using the same procedure, differing only in the metal precursor employed.

2.3 Characterization Techniques

The morphological and structural features of the synthesized samples were examined using transmission electron microscopy (TEM and HRTEM), which provided information on particle size, lattice fringes, and crystallinity. Fourier transform infrared spectroscopy (FTIR) was employed to identify metal–oxygen vibrations and surface functional groups. Raman spectroscopy was used to analyze phonon modes and lattice interactions in the individual oxides and the ZnO/NiO composite. Photoluminescence (PL) spectroscopy was carried out to study band-edge emission, defect states, and charge-recombination behavior of the nanomaterials.

3. Results and discussion

3.1. TEM Analysis of ZnO, NiO and ZnO/NiO

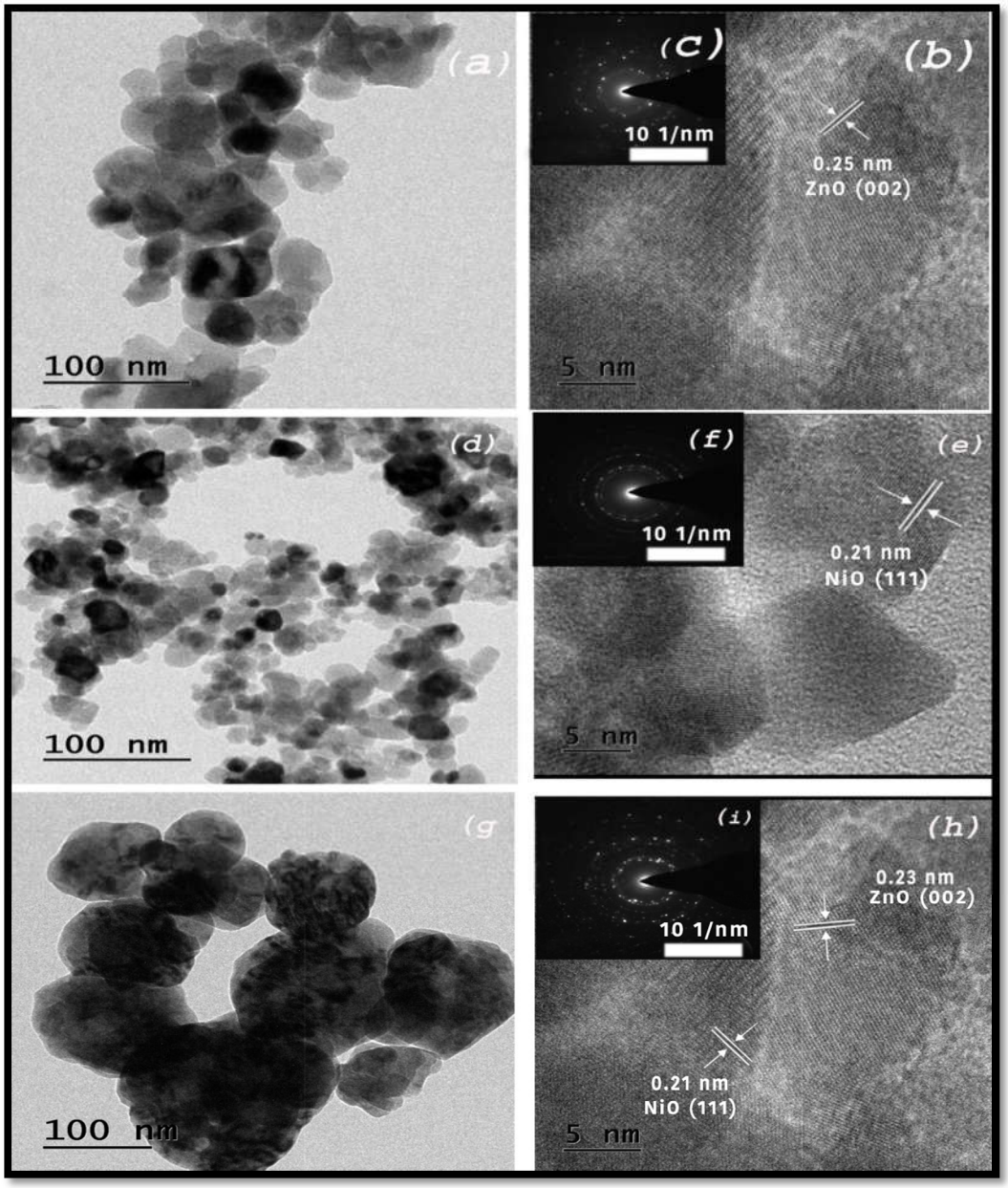

Figure 3.1: TEM, HRTEM, and SAED characterization of (a–c) ZnO, (d–f) NiO, and (g–i) ZnO/NiO nanocomposite samples.

The structural features of the green-synthesized ZnO, NiO, and ZnO/NiO nanomaterials were comprehensively examined using TEM, HRTEM, and SAED, as presented in Fig. 3.1 (a–i). The TEM micrograph of ZnO (Fig. 3.1 a) reveals aggregated nanosized particles with uneven yet well-separated domains, a morphology commonly observed for bio-mediated ZnO where phytochemicals regulate nucleation and restrict extreme particle growth. The corresponding

HRTEM image (Fig. 3.1 b) displays lattice fringes with a spacing of 0.25 nm, which can be indexed to the (002) plane of hexagonal wurtzite ZnO, confirming its crystalline nature and consistent with earlier reported values for green-synthesized ZnO nanostructures [6]. The polycrystalline nature is further supported by the SAED pattern (Fig. 3.1 c), which shows multiple sharp diffraction rings corresponding to standard ZnO reflections. The TEM image of NiO (Fig. 3.1 d) shows smaller, more uniformly dispersed nanoparticles, indicative of the effective capping action of plant-derived biomolecules during nucleation and growth. The HRTEM image (Fig. 3.1 e) exhibits a well-resolved lattice fringe of 0.21 nm, attributed to the (111) plane of cubic NiO, in agreement with previous studies on biogenic NiO nanoparticles [7]. The SAED pattern (Fig. 3.1 f) confirms the crystallinity of NiO through concentric rings characteristic of the FCC structure. In the case of the ZnO/NiO nanocomposite (Fig. 3.1 [g–i]), the TEM micrograph displays dense clusters composed of both ZnO and NiO domains, suggesting strong interparticle fusion induced during co-nucleation in the plant extract. The HRTEM micrograph (Fig. 3.1 h) distinctly reveals two sets of lattice fringes: 0.23 nm, corresponding to ZnO (002), and 0.21 nm, corresponding to NiO (111), confirming the formation of a ZnO/NiO heterojunction where both phases are intimately interfaced. Such nanointerfaces are known to promote efficient electron–hole separation and facilitate interfacial charge migration, which is advantageous for photocatalytic and energy-related applications [8,9]. The presence of diffraction features from both ZnO and NiO in the SAED pattern (Fig. 3.1 i) further substantiates the biphasic crystalline nature of the composite [4,10]. The microstructural characteristics observed here align with earlier reports demonstrating that green synthesis pathways can yield high-crystallinity metal-oxide nanoparticles and well-defined heterostructures suitable for advanced functional applications [14-16].

3.2 Vibrational analysis of ZnO, NiO, and ZnO/NiO

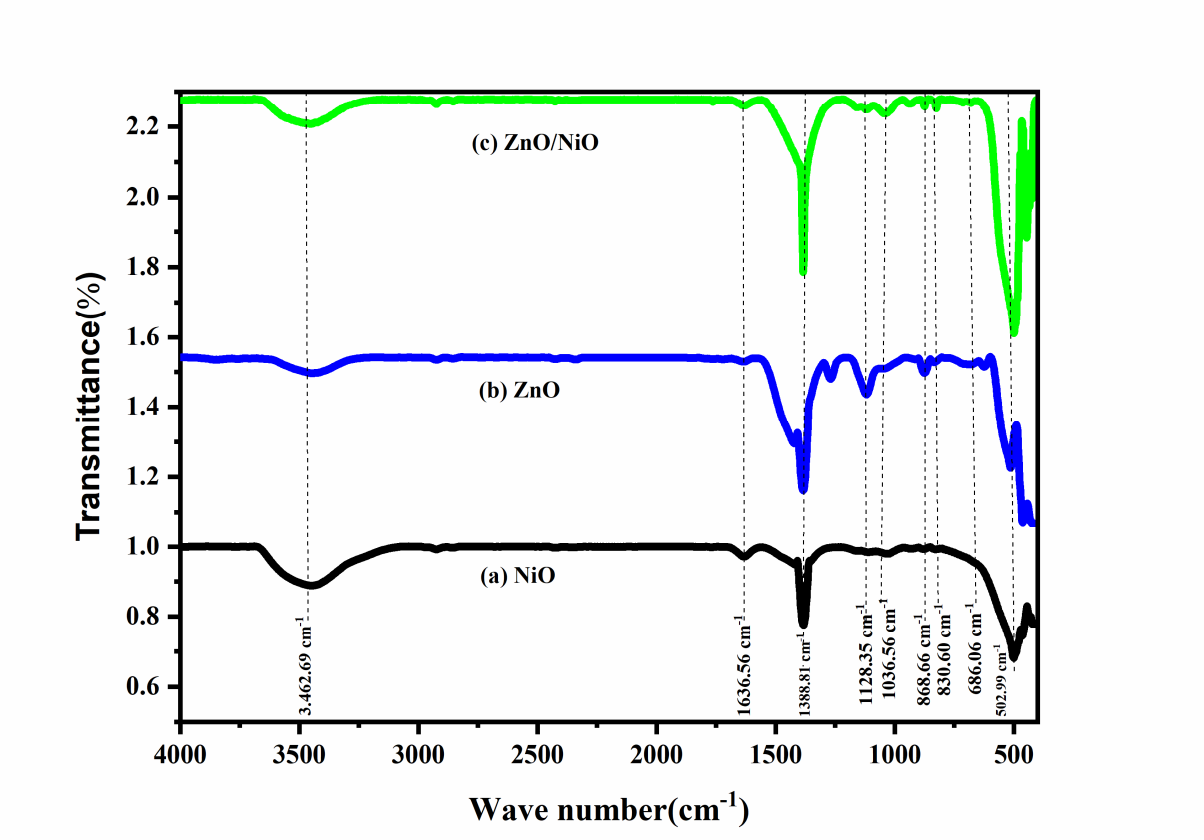

Figure 3.2: FTIR spectra confirming Zn–O, Ni–O vibrations and composite phase integration.

The FTIR spectra of the green-synthesized NiO, ZnO, and ZnO/NiO nanocomposite exhibit characteristic vibrational features that reflect the presence of metal–oxygen frameworks and surface functional groups originating from the plant extract used in the synthesis as shown in Figure 3.2. In the spectrum of NiO, a prominent absorption band observed below 600 cm^{-1} corresponds to the fundamental stretching vibration of Ni–O bonds in the cubic NiO lattice, in agreement with typical metal–oxygen phonon modes reported for biogenic NiO nanoparticles [7]. Additional low-intensity features around 3400 cm^{-1} are associated with O–H stretching vibrations from physically adsorbed water or residual phytochemicals, a common signature in green-synthesized metal oxides due to the presence of hydroxyl-rich biomolecules [4]. The FTIR spectrum of ZnO displays a strong metal–oxygen vibrational band in the region of 400–500 cm^{-1}, confirming the formation of Zn–O bonds characteristic of hexagonal wurtzite ZnO [6]. Minor absorption features between 1000 and 1600 cm^{-1} can be attributed to C–O, C=O, and C–N stretching vibrations, which arise from organic residuals of the plant extract that act as chelating and stabilizing species during nanoparticle formation [10].

In the case of the ZnO/NiO nanocomposite, the FTIR spectrum exhibits combined vibrational bands of both Zn–O and Ni–O species, validating the simultaneous incorporation of both metal oxides within the nanostructure. The metal–oxygen band becomes slightly broader and more intense, suggesting synergistic interactions between ZnO and NiO domains and possible modification of bond environments at the heterojunction interface. Similar band broadening and merging effects have been reported for ZnO/NiO hybrid structures, where interface formation alters local lattice symmetry and enhances vibrational coupling between the two oxide phases [8,9]. Notably, the reduced intensity of hydroxyl-related bands in the composite indicates improved crystallinity, a result of thermal decomposition of organic constituents during calcination. Such observations are consistent with earlier studies that demonstrated the ability of green synthesis routes to produce crystalline mixed-metal oxides with diminished organic residue after heat treatment [17-19]. Overall, the FTIR spectra confirm the formation of phase-pure ZnO and NiO as well as their successful integration into a ZnO/NiO heterostructure, highlighting the effectiveness of plant-mediated synthesis in enabling metal–oxygen lattice formation and interfacial interactions favorable for energy-related applications.

3.3 Raman Spectra of ZnO, NiO and ZnO/NiO

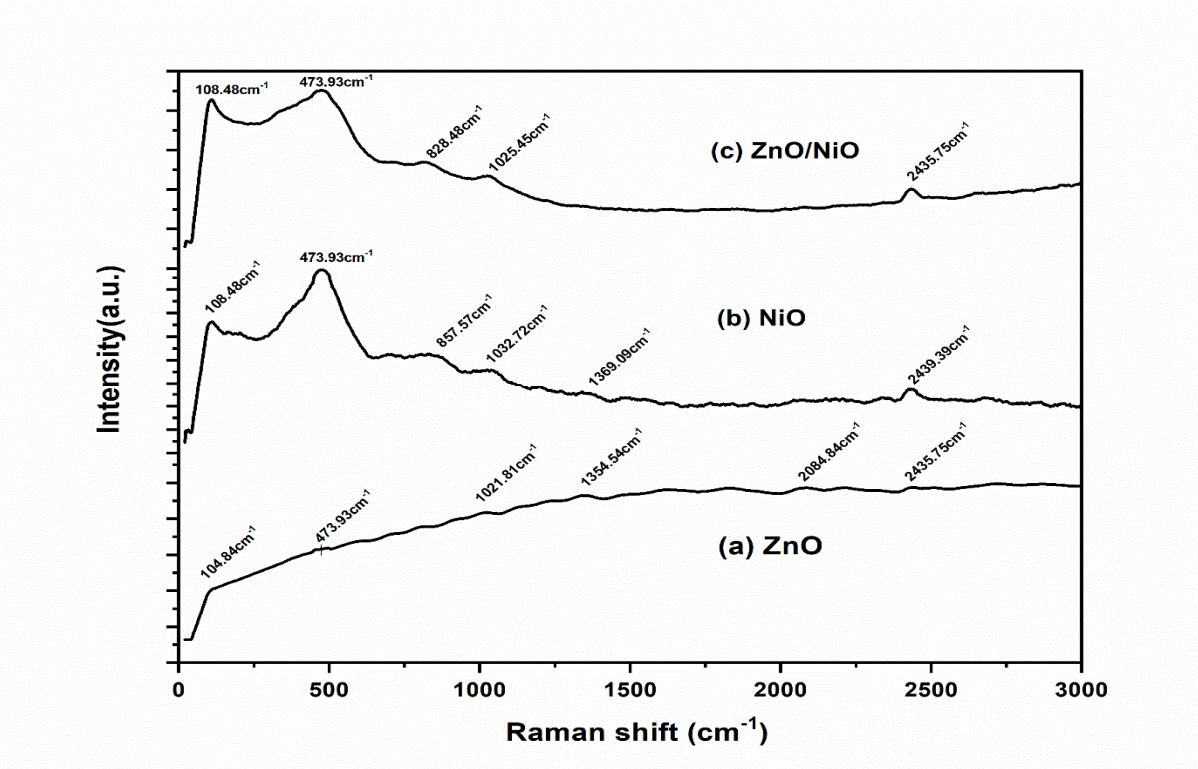

Figure 3.3: Raman spectra showing characteristic ZnO and NiO modes and interfacial phonon coupling.

The Raman spectra of the green-synthesized ZnO, NiO, and ZnO/NiO nanocomposite display distinct vibrational signatures associated with their respective crystal structures, providing crucial insight into phonon behavior, structural disorder, and heterojunction formation as shown in Figure 3.3. The spectrum of ZnO shows two prominent modes at approximately 108–110 cm^{-1} and 473–475 cm^{-1}, corresponding to the $E_2(low)$ and $E_2(high)$ phonon modes of hexagonal wurtzite ZnO, respectively—both of which are characteristic Raman-active vibrations of high-quality ZnO nanocrystals [11]. The $E_2(high)$ mode, observed near 474 cm^{-1}, is particularly sensitive to oxygen sublattice vibrations and is often used as an indicator of crystallinity, with the strong, sharp peak confirming the well-ordered ZnO lattice obtained via green synthesis [6]. Additional weak and broad features in the 1000–1500 cm^{-1} region may be associated with multi-phonon scattering or defect-induced vibrational activity, typically attributed to intrinsic oxygen vacancies, zinc interstitials, or surface-state perturbations introduced during biosynthesis [10].

The Raman spectrum of NiO is dominated by a set of broader bands, including features at ~857, 1032, 1359, and 2439 cm^{-1}, which arise from one-phonon and two-phonon processes of cubic NiO. The first-order Raman signal in NiO is symmetry-forbidden in perfect FCC structures; however, nanoscale NiO commonly exhibits these features due to lattice defects, phonon confinement, and nonstoichiometric Ni^{3+}/Ni^{2+} centers—all of which activate silent modes [12]. The peaks above 1000 cm^{-1} correspond to second-order longitudinal optical (2LO) and transverse optical (2TO) modes, consistent with previously reported Raman behavior of nanocrystalline NiO synthesized through plant-mediated or soft-chemical routes [7].

In the ZnO/NiO nanocomposite, the Raman spectrum exhibits vibrational contributions from both ZnO and NiO, confirming successful hybridization of the two oxide phases. The E_2 modes of ZnO remain identifiable but show slight shifts and broadening, indicating lattice strain and phonon coupling at the ZnO–NiO interface. Simultaneously, the characteristic NiO modes persist but with modified intensities, reflecting interfacial charge redistribution and structural distortion induced by the formation of the p–n heterojunction [8]. Such phonon mode shifts and intensity changes are widely considered evidence of strong vibrational coupling in mixed-metal oxide nanocomposites, demonstrating altered phonon lifetimes and enhanced carrier

interaction across the interface [9]. The coexistence of Raman signatures from both oxides, combined with their spectral modifications, reinforces the successful formation of the ZnO/NiO heterostructure and highlights the influence of green synthesis on defect formation, phonon confinement, and interfacial bonding [20-22].

3.4 Photoluminescence of ZnO, NiO and ZnO/NiO

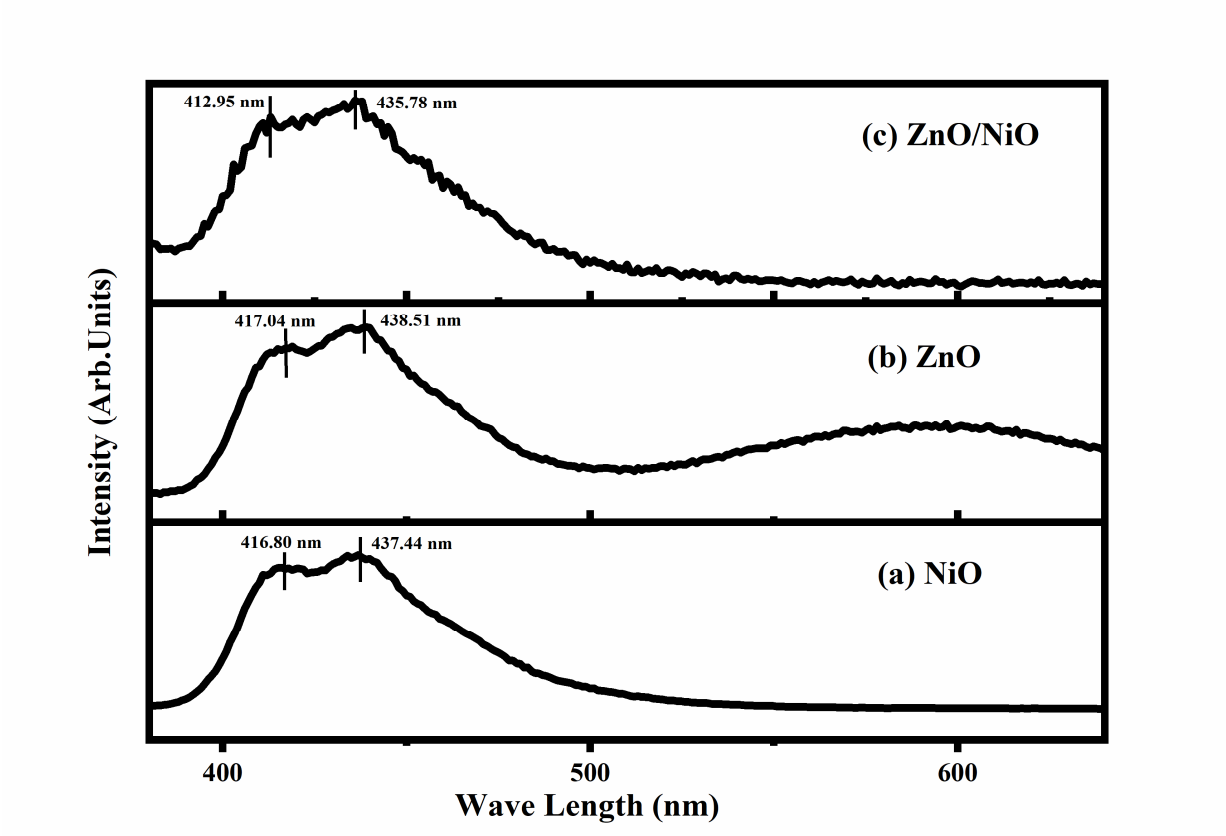

Figure 3.4: PL spectra showing defect emissions and reduced recombination in the ZnO/NiO composite.

The photoluminescence (PL) spectra of NiO, ZnO, and the ZnO/NiO nanocomposite provide valuable insights into the electronic transitions, defect states, and interfacial charge-transfer behavior of the green-synthesized materials. The NiO spectrum (Fig. 3.4 a) exhibits two emission peaks centered at approximately 416.8 nm and 437.4 nm, which are attributed to defect-mediated electronic transitions involving Ni^{2+}/Ni^{3+} centers and oxygen vacancy–related states within the cubic NiO lattice. Such emissions are characteristic of nanostructured NiO, where size confinement and surface defects activate visible-region luminescence [12]. The broad emission tail extending into the visible region is primarily associated with recombination

between localized defect levels and the valence band, a behavior commonly reported for NiO nanoparticles synthesized via plant-based routes [7].

The ZnO spectrum (Fig. 3.4 b) shows two major emission peaks at 417.0 nm and 438.5 nm, corresponding to the near-band-edge (NBE) excitonic recombination and deep-level emission (DLE), respectively. The NBE peak around 417 nm arises from the recombination of free excitons in the wurtzite ZnO lattice, confirming its high crystallinity, [2] while the DLE peak near 438 nm originates from intrinsic point defects such as oxygen vacancies (V_o), zinc interstitials (Zn_i), and surface states—defects typically enhanced under biosynthesis due to organic functional groups acting as mild reducing agents [6]. The broad visible emission background also indicates the presence of multiple defect-related transitions, a common signature in green-synthesized ZnO nanostructures [10].

The ZnO/NiO nanocomposite (Fig. 3.4 c) displays emission peaks at 412.9 nm and 435.8 nm, showing a slight blue shift compared to those of the individual oxides. This spectral shift is indicative of strong interfacial coupling between the p-type NiO and n-type ZnO phases, which modifies local band energies and enhances exciton–phonon interactions. The overall PL intensity of the composite is significantly reduced relative to pure ZnO, demonstrating suppressed electron–hole recombination due to efficient charge separation at the p–n heterojunction interface [8]. Lower PL intensity is widely recognized as a marker of improved charge-transfer efficiency, particularly beneficial for photocatalysis and energy-storage applications [9]. The presence of both NBE and DLE emissions further confirms that the composite retains the intrinsic optical transitions of the parent oxides while benefiting from enhanced interfacial charge dynamics [13]. These observations are consistent with earlier reports that ZnO/NiO heterostructures exhibit reduced PL intensity and band-edge shifts due to interfacial electronic redistribution within the heterojunction [23-25].

Overall, the PL spectra demonstrate that the green-synthesized ZnO/NiO nanocomposite exhibits modified optical behavior arising from strong interfacial charge transfer, reduced recombination, and altered defect-state dynamics, all of which contribute to enhanced suitability for optoelectronic and energy-related applications.

4. Conclusion

The structural and optical analyses carried out using TEM, FTIR, Raman, and PL collectively confirm the successful green synthesis of ZnO, NiO, and the ZnO/NiO nanocomposite and provide strong evidence for the formation of a well-defined heterojunction. TEM and HRTEM

images revealed nanoscale morphologies with distinct lattice fringes corresponding to ZnO (002) and NiO (111) planes, while SAED patterns demonstrated high crystallinity and clear coexistence of both oxide phases in the composite. FTIR spectra validated the presence of characteristic Zn–O and Ni–O vibrational modes, along with reduced organic signatures in the composite, indicating effective phase formation and improved structural integrity. Raman spectroscopy further supported this by showing the expected phonon modes of ZnO and NiO, with the composite displaying combined and slightly shifted bands due to interfacial vibrational coupling. Photoluminescence studies showed that the ZnO/NiO composite exhibits blue-shifted emission peaks and significantly reduced PL intensity, demonstrating enhanced charge separation and suppressed electron–hole recombination within the heterostructure. Altogether, these results confirm that the green-synthesized ZnO/NiO nanocomposite possesses improved structural order, strong interfacial bonding, and superior optical charge-transfer behavior, making it a promising candidate for advanced energy-related and optoelectronic applications.

Credit author statement

Akumarti Raju: Conceptualization, Methodology, Formal analysis, Investigation, Writing – original draft. **Vangapandu Anusha:** Data curation, Investigation. **Budithi Ravi Kumar:** Data curation, Investigation. **Gattupalli Manikya Rao:** Data curation, Formal analysis, Investigation, Supervision. **Vangapandu Anusha 1:** Formal analysis, Conceptualization. **Akumarti Raju 1:** Conceptualization, Investigation, Methodology, Writing – review & editing.

Declaration of competing interest

The authors declare that they have no known competing financial interests or personal relationships that could have appeared to influence the work reported in this paper.

Data Availability Statement

The original contributions presented in the study are included in the article/Supplementary Material. Further inquiries can be directed to the corresponding author.

Acknowledgment

The authors acknowledge the Department of Physics, Andhra University, for providing the necessary facilities.

REFERENCES

1. Henderson, M. A. *A Surface Science Perspective on TiO_2 Photocatalysis.* Prog. Solid State Chem. 2013, 41, 3–15. https://doi.org/10.1016/j.progsolidstchem.2013.03.001
2. Özgür, Ü.; Alivov, Y. I.; Liu, C.; Teke, A.; Reshchikov, M. A.; Doğan, S.; Avrutin, V.; Cho, S.-J.; Morkoç, H. *A Comprehensive Review of ZnO Materials and Devices.* J. Appl. Phys. 2005, 98, 041301.https://doi.org/10.1063/1.1992666
3. Li, X.; Xiong, J.; Xu, Y.; Feng, Z.; Huang, J.; Zhou, C. *ZnO/NiO p–n Heterojunction Nanocomposites for Enhanced Photocatalytic Activity under Visible Light.* Chem. Eng. J. 2017, 315, 376–384. https://doi.org/10.1016/j.cej.2017.01.099
4. Iravani, S. *Green Synthesis of Metal Nanoparticles Using Plants.* Green Chem. 2011, 13, 2638–2650. https://doi.org/10.1039/C1GC15386B
5. Sivakumar, V.; Suresh, R.; Giribabu, K.; Narayanan, V.; Stephen, A. *Enhanced Photoluminescence and Charge Transfer Properties of ZnO/NiO Nanocomposites.* Opt. Mater. 2019, 94, 109915. https://doi.org/10.1016/j.optmat.2019.109915
6. Baruah, S.; Dutta, J. *Hydrothermal Growth of ZnO Nanostructures.* Sci. Technol. Adv. Mater. 2009, 10, 013001. https://doi.org/10.1088/1468-6996/10/1/013001
7. Sutradhar, P.; Saha, M.; Maiti, D. *Microwave-Assisted Green Synthesis of NiO Nanoparticles Using Tea Extract and Their Catalytic Activity.* J. Nanostruct. Chem. 2014, 4, 1–6. https://doi.org/10.1007/s40097-014-0102-x
8. Singh, G.; et al. *Facile Synthesis of ZnO/NiO Nanocomposites and Their Photocatalytic Properties.* ACS Omega 2019, 4, 11369–11379. https://doi.org/10.1021/acsomega.9b01087
9. Umar, A.; et al. *Synthesis and Characterization of ZnO/NiO Nanocomposite for Photocatalytic Applications.* J. Alloys Compd. 2015, 649, 443–450. https://doi.org/10.1016/j.jallcom.2015.03.155
10. Mishra, A.; Mehdi, M.; Chauhan, P. *Green Synthesis of Zinc Oxide Nanoparticles Using Plant Extracts: A Sustainable Approach.* Mater. Lett. 2022, 315, 131999. https://doi.org/10.1016/j.matlet.2021.131999
11. Cuscó, R.; et al. *Temperature Dependence of Raman Scattering in ZnO.* Phys. Rev. B 2007, 75, 165202. https://doi.org/10.1103/PhysRevB.75.165202
12. Balaji, S.; et al. *Raman Spectroscopy of Nanostructured NiO: Phonon Confinement and Defect-Induced Modes.* J. Phys. Chem. C 2010, 114, 15853–15858. https://doi.org/10.1021/jp105087b

13. Chen, X.; Mao, S. S. *Titanium Dioxide Nanomaterials: Synthesis, Properties, Modifications, and Applications.* Chem. Rev. 2007, 107, 2891–2959. https://doi.org/10.1021/cr0500535.
14. Wang, Z. L. *Transmission Electron Microscopy of Shape-Controlled Nanocrystals and Their Assemblies.* J. Phys. Chem. B 2000, 104, 1153–1175. https://doi.org/10.1021/jp993593c
15. Zhang, Y.; Nayak, T. R.; Hong, H.; Cai, W. *Biomedical Applications of Zinc Oxide Nanomaterials.* Curr. Mol. Med. 2013, 13, 1633–1645. https://doi.org/10.2174/15665240136661311111130051
16. Kumar, V.; Kumar, S.; Saini, P.; Malik, H. K. *Structural and Morphological Properties of NiO Nanoparticles Synthesized by Chemical Route.* Ceram. Int. 2014, 40, 8411–8418. https://doi.org/10.1016/j.ceramint.2014.01.083
17. Coates, J. *Interpretation of Infrared Spectra, A Practical Approach.* Encyclopedia of Analytical Chemistry; Wiley, 2000. https://doi.org/10.1002/9780470027318.a5606
18. Jayachandran, M.; Vijayaprasath, G.; Sankari, G.; Ravi, G. *Effect of Capping Agent on Structural and Optical Properties of ZnO Nanoparticles.* Spectrochim. Acta A 2016, 152, 680–686. https://doi.org/10.1016/j.saa.2015.07.049
19. Vangapandu Anusha, Budithi Ravi Kumar. "Eco-Friendly Fabrication and Electrochemical Evaluation of Mn_2O_3, CuO, and Mn_2O_3/CuO Nanocomposite for Energy Storage Applications." *International Journal of Applied Mathematics*. Volume 38 No. 8, 2025. DOI: https://doi.org/10.12732/ijam.v38i8s.935.
20. Calleja, J. M.; Cardona, M. *Resonant Raman Scattering in ZnO.* Phys. Rev. B 1977, 16, 3753–3761. https://doi.org/10.1103/PhysRevB.16.3753
21. Reich, S.; Ferrari, A. C. *Resonant Raman Scattering in Semiconductor Nanostructures.* Phys. Rev. B 2005, 71, 205201. https://doi.org/10.1103/PhysRevB.71.205201
22. Alim, K. A.; Fonoberov, V. A.; Balandin, A. A. *Origin of Optical Phonons in ZnO Quantum Dots.* Appl. Phys. Lett. 2005, 86, 053103. https://doi.org/10.1063/1.1855423
23. Vanheusden, K.; Warren, W. L.; Seager, C. H.; Tallant, D. R.; Voigt, J. A.; Gnade, B. E. *Mechanisms Behind Green Photoluminescence in ZnO Phosphor Powders.* J. Appl. Phys. 1996, 79, 7983–7990. https://doi.org/10.1063/1.361491
24. Djurišić, A. B.; Leung, Y. H. *Optical Properties of ZnO Nanostructures.* Small 2006, 2, 944–961. https://doi.org/10.1002/smll.200600134

25. Zhu, H.; Yang, D.; Yu, G.; Zhang, H.; Yao, K. *Photoluminescence and Optical Properties of NiO Nanoparticles.* Physica B 2005, 364, 199–204. https://doi.org/10.1016/j.physb.2005.03.028